A

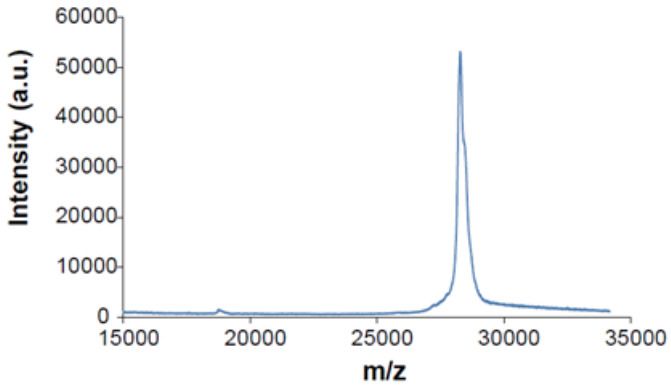

B

>Repebody rEgA

```
       10         20         30         40         50         60
METITVSTPI KQIFPDDAFA ETIKANLKKK SVTDAVTQNE LNSIDQIIAN NSDIKSVQGI

       70         80         90        100        110        120
QYLPNVRYLA LGGNKLHDIS ALKELTNLTY LMLHYNQLQI LPNGVFDKLT NLKELYLSEN

      130        140        150        160        170        180
QLQSLPDGVF DKLTNLTELD LARNQLQSLP KGVFDKLTQL KDLRLYENQL KSVPDGVFDR

      190        200        210        220        230        240
LTSLQYIWLH DNPWDCTCPG IRYLSEWINK HSGVVRNSAG SVAPDSAKCS GSGKPVRSII

      250
CPTELHHHHH H

Theoretical pI/Mw: 6.54 / 28269.22
```

Figure S1. Matrix assisted laser desorption/ionization time-of-flight (MALDI-TOF) mass spectra of repebody rEgA (A) and complete amino acid sequence of the repebody rEgA (B). (A) Mass spectra of rEgA presented in the mass-to-charge (m/z) range to 15 to 35 kDa. Measured peak is displayed with corresponding molecular mass. (B) The molecular weight of rEgA was calculated by using Expasy Compute pI/Mw tool.

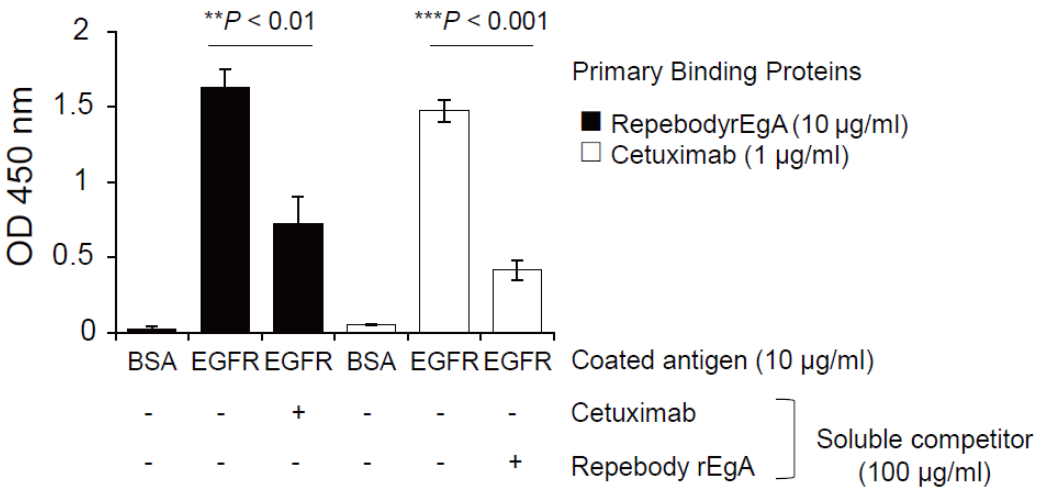

Figure S2. Competitive ELISA for prediction of the binding epitope of the repebody rEgA on EGFR. For competition analysis, the repebody rEgA and cetuximab were co-incubated with an excess of soluble cetuximab and the repebody rEgA, respectively. The signal was measured at 450 nm. BSA was used as a negative control.

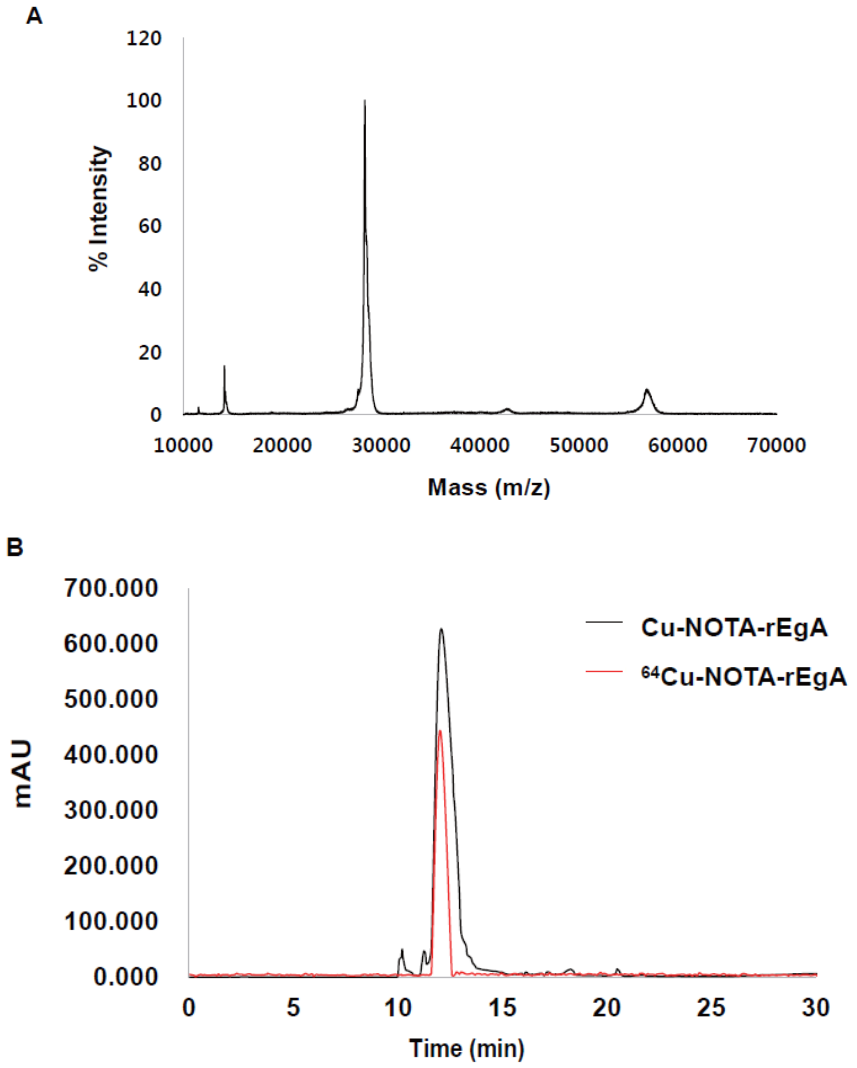

Figure S3. MALDI-TOF mass spectra of NOTA-rEgA (A) and HPLC chromatogram of Cu-NOTA-rEgA / ^{64}Cu-NOTA-rEgA (B). (A) Mass spectra of rEgA presented in the mass-to-charge (m/z) range to 10 to 70 kDa. Measured peaks are displayed with corresponding molecular mass. (B) Absorbance of Cu-NOTA-rEgA was measured at 218 nm (black line) and red line showed the radioactivity of ^{64}Cu-NOTA-rEgA.

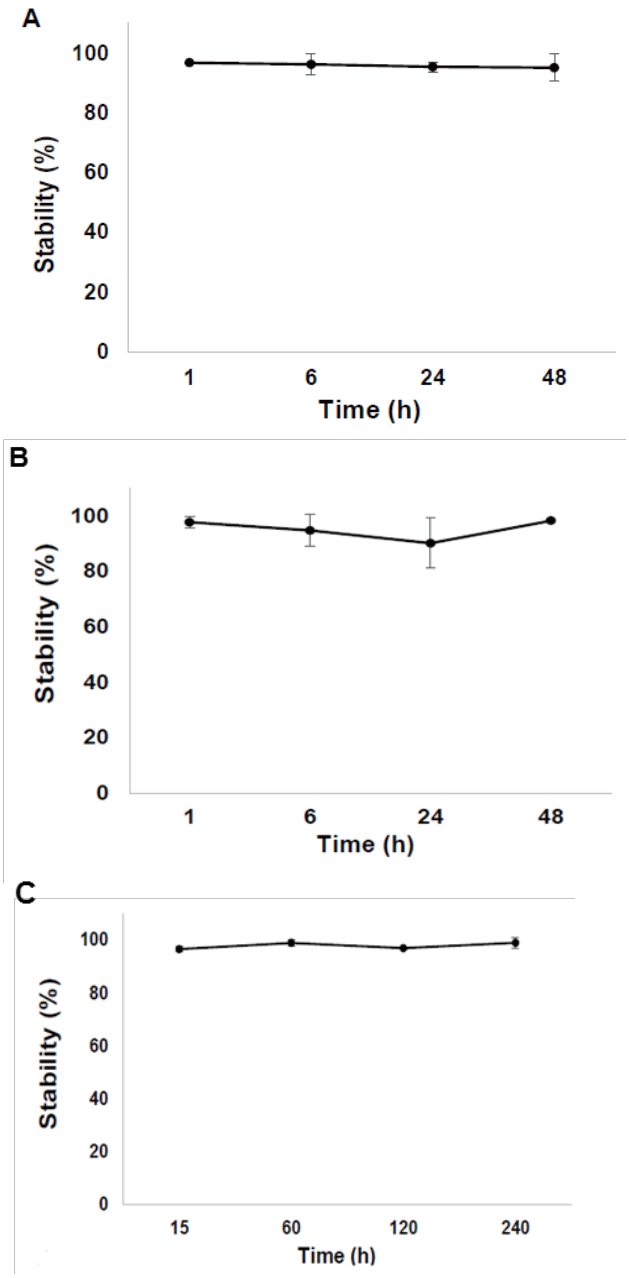

Figure S4. Stability test of ^{64}Cu-NOTA-rEgA *in vitro* (A), *in vitro* with excess of EDTA (B), *in vivo* (C). *In vitro* stability test without or with excess of EDTA (10 eq) was performed at 37°C for 48h. *In vivo* stability test was performed for 4 h. ^{64}Cu-NOTA-rEgA was greater than 95%, indicating a relatively high *in vitro* / *in vivo* stability.

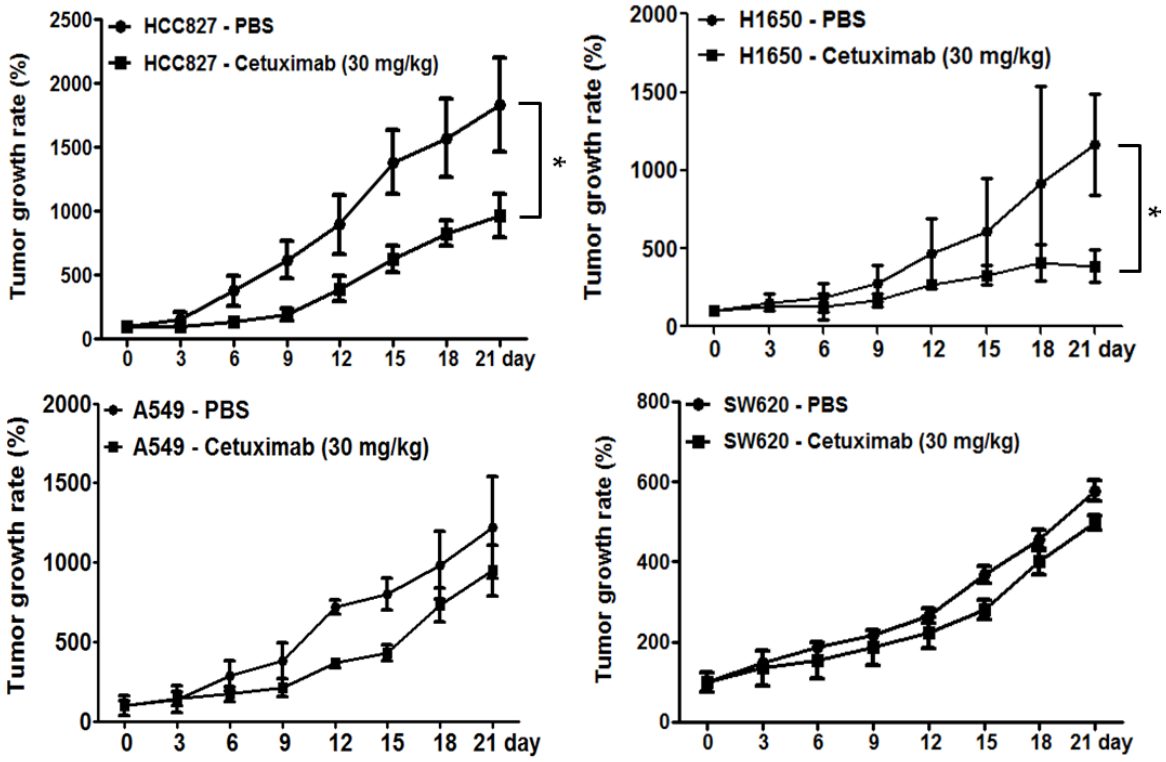

Figure S5. Susceptibility of tumors (HCC827, H1650, A549, and SW620) grafted into mice. Tumor-bearing mice (n = 5 per condition) were intraperitoneally treated with 30 mg/kg cetuximab, twice a week for 4 weeks. The treatment was initiated when the tumor size was approximately 100 mm^3. Tumor volume was measured on the indicated days. (* $P < 0.001$)

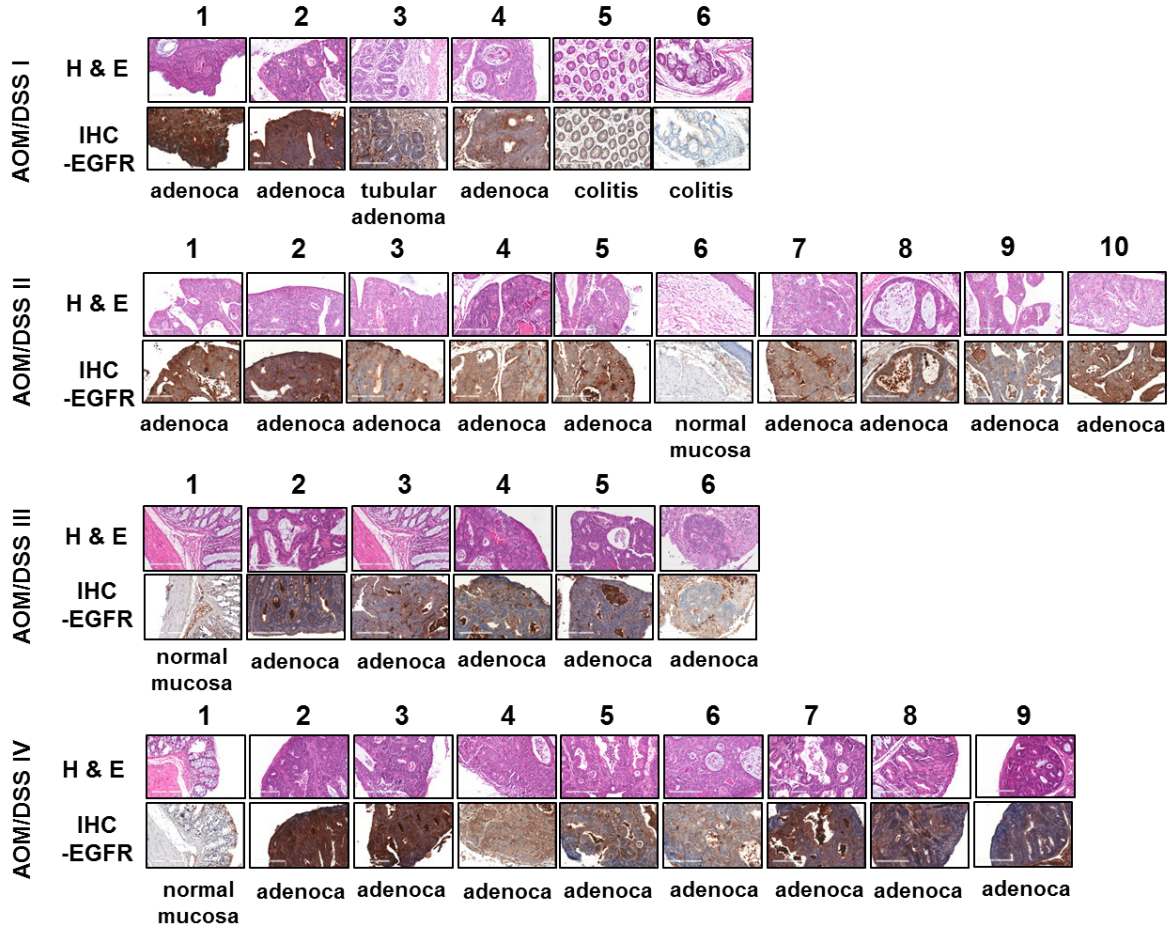

Figure S6. Hematoxylin and eosin (H & E) and immunohistochemical (IHC) staining of excised colon cancers from AOM/DSS models. EGFR expression of colonic cancers was assessed by IHC staining using an EGFR-specific antibody. Adenoca: Adenocarcinoma

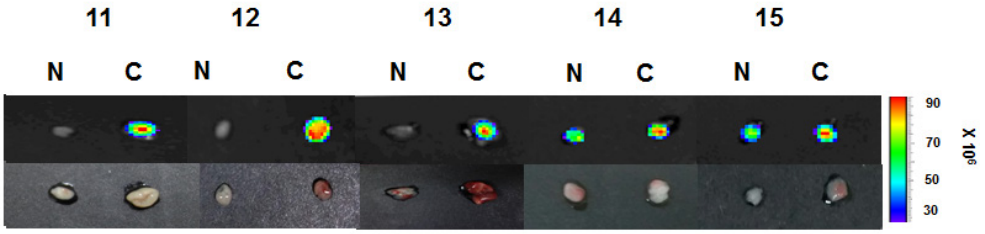

Figure S7. rEgA *ex vivo* stain of human cancer tissue. Human colon cancer and normal mucosa tissues were stained *ex vivo* with rEgA-675 (case 11-15). N: Normal mucosa or colitis, C: Dysplasia or Adenocarcinoma.

Table S1. Quantitation of the protein-dye conjugation by absorbance measurements

Protein-fluorophore conjugate	A_{max}	A_{280}	ε	CF	ε'	Protein concentration (M)	Moles of dye per mole protein (F/P molar ratio)
rEgA-675	0.24	0.045	28920	0.09	220000	0.00000081	1.3483
rEgA-496	0.096	0.071	28920	0.35	84000	0.00000129	0.8837
Cetuximab-675	0.109	0.063	109720	0.09	220000	0.00000048	1.0220

A_{max} = Absorbance (A) of a dye solution measured at the wavelength maximum (λ_{max}) for the dye molecule.

A_{280} = Absorbance at 280 nm (A280).

ε = Protein molar extinction coefficient.

CF = Correction factor; adjusts for the absorbance by the dye at 280 nm.

ε′ = Molar extinction coefficient of the fluorescent dye.

$$\text{Protein concentration (M)} = \frac{A280-(Amax \times CF)}{\varepsilon} \times \text{dilution factor}$$

$$\text{Moles of dye per mole protein} = \frac{\text{Amax of the labeled protein}}{\varepsilon' \times \text{protein concentration (M)}} \times \text{dilution factor}$$

Table S2. Comparison of tumor-to-muscle, tumor-to-blood and tumor-to-liver uptake ratios of HT-29, H1650 (high expression of EGFR) and A549 (moderate expression of EGFR) tumors of ^{64}Cu-NOTA-rEgA at 1, 6, 24 and 48 h post-injection.

	Tumor-to-muscle				
	HT-29	HT-29 block	H1650	H1650 block	A549
1 h	15.43 ± 1.96	3.80 ± 0.27	15.04 ± 4.41	6.38 ± 2.59	6.52 ± 0.80
6 h	18.73 ± 4.49†¶	3.68 ± 0.83¶	23.18 ± 3.14*†¶	7.48 ± 2.68	6.90 ± 0.75†¶
24 h	10.95 ± 1.01	4.45 ± 0.55	13.33 ± 3.25	9.47 ± 2.75	3.64 ± 0.68
48 h	10.55 ± 0.43	5.27 ± 0.96	10.21 ± 2.16	10.06 ± 1.26	3.21 ± 0.78
	Tumor-to-blood				
	HT-29	HT-29 block	H1650	H1650 block	A549
1 h	4.72 ± 0.70	1.03 ± 0.09	4.27 ± 1.11	1.82 ± 0.11	1.76 ± 0.15
6 h	5.01 ± 1.03†	0.83 ± 0.18†¶	5.01 ± 0.85¶	1.86 ± 0.12†¶	1.16 ± 0.05*†¶
24 h	3.53 ± 0.54	1.20 ± 0.19	4.01 ± 1.19	2.79 ± 0.51	0.81 ± 0.18
48 h	3.73 ± 0.78	1.86 ± 0.59	2.72 ± 0.57	3.02 ± 0.69	1.00 ± 0.11
	Tumor-to-liver				
	HT-29	HT-29 block	H1650	H1650 block	A549
1 h	0.50 ± 0.07	0.13 ± 0.01	0.45 ± 0.08	0.16 ± 0.04	0.14 ± 0.02
6 h	0.64 ± 0.16	0.17 ± 0.04†¶	0.67 ± 0.67*	0.34 ± 0.15*¶	0.18 ± 0.02*
24 h	0.51 ± 0.14	0.24 ± 0.03	0.69 ± 0.69	0.53 ± 0.17	0.14 ± 0.04
48 h	0.56 ± 0.14	0.35 ± 0.07	0.70 ± 0.70	0.62 ± 0.15	0.20 ± 0.08

Data was expressed mean ± SD. $^{*}P < 0.05$ vs. value at 1 h, $^{\dagger}P < 0.05$ vs. value at 24 h, $^{\P}P < 0.05$ vs. value at 48 h

Table S3. Biodistribution of ^{64}Cu-NOTA-rEgA.

	1 h	6 h	24 h
Blood	2.78 ± 0.37	2.61 ± 0.46	2.33 ± 0.29
Heart	5.23 ± 0.55	5.03 ±0.92	4.52 ± 0.17
Lung	5.05 ± 1.19	5.83 ± 2.0	4.91 ± 0.98
Liver	14.21 ± 0.80	15.33 ± 0.97	16.61 ± 1.99
Spleen	3.82 ± 0.18	3.98 ± 0.17	4.20 ± 0.12
Stomach	2.59 ± 0.54	3.12 ± 1.2	3.40 ± 0.80
Intestine	11.79 ±0.23	7.73 ±0.43*†	5.52 ± 0.61
Kidney	20.42 ±0.89	13.94 ± 1.48*	13.79 ± 3.02
Pancreas	3.31 ±0.19	3.29 ± 0.66	2.21 ± 0.18
Normal muscle	1.00 ±0.13	0.87 ± 0.14	0.82 ± 0.18
Bone	2.07 ± 0.98	2.19 ± 0.47	1.81 ± 0.20
Brain	0.40 ± 0.06	0.46 ± 0.06	0.59 ± 0.01
Skin	4.94 ± 0.27	3.20 ± 0.52*	2.53 ± 0.49
Tumor	10.56 ± 1.55	14.31 ± 2.68*†	7.89 ± 2.61
Tumor-to-blood	3.80 ± 0.07	5.47 ± 0.16*	3.52 ± 1.90
Tumor-to-muscle	10.51 ± 0.28	16.50 ± 1.59*†	9.30 ± 2.19
Tumor-to-liver	0.75 ± 0.13	0.94 ± 0.18	0.50 ± 0.29

^{64}Cu-NOTA-rEgA injected into mice bearing implanted H1650 xenografts, as determined by γ-counting. Values are mean and standard deviation (n = 6). $^{*}P < 0.05$ vs. value at 1 h, $^{\dagger}P < 0.05$ vs. value at 24 h

Table S4. Characteristics and Pathologic data of human *ex vivo* rEgA-stained cancer tissues.

Case	Location of tumor	Stage and Lesion Characteristics	Treatment	Pathology
1	Sigmoid colon	Advanced, T4N2M1	Surgery + Chemotherapy	Adenocarcinoma, moderately differentiated
2	Sigmoid colon	Advanced, T4N2M0	Surgery + Chemotherapy	Adenocarcinoma, moderately differentiated
3	Ascending colon	Benign sessile polyp, 15mm	Endoscopic resection	Tubular adenoma with low grade dysplasia
4	Rectum	Advanced, T4N2M1	Chemotherapy	Adenocarcinoma, poorly differentiated
5	Rectosigmoid junction	Advanced, T3N1M0	Surgery + Chemotherapy	Adenocarcinoma, moderately differentiated
6	Sigmoid colon	Advanced, T3N3M1	Chemotherapy	Adenocarcinoma, moderately differentiated
7	Sigmoid colon	Advanced, T3N0M1	Surgery + Chemotherapy	Adenocarcinoma, well differentiated
8	Cecum	Early, Malignant polyp, 28mm	Endoscopic resection	Adenocarcinoma, well differentiated
9	Ascending colon	Benign, pedunculated polyp, 15mm	Endoscopic resection	Hyperplastic polyp
10	Hepatic flexure	Advanced, T2N0M0	Surgery	Adenocarcinoma with papillary feature, well differentiated
11	Rectum	Advanced, T3N0M0	Surgery	Adenocarcinoma, poorly differentiated
12	Sigmoid colon	Early malignant polyp, 25mm	Endoscopic resection	Adenocarcinoma, well differentiated
13	Rectum	Early malignant polyp, 20mm	Endoscopic resection	Tubular adenoma with High grade dysplasia
14	Sigmoid colon	Advanced, T3N0M0	Surgery	Adenocarcinoma, moderately differentiated
15	Sigmoid colon	Early malignant polyp, 30mm	Endoscopic resection	Tubulovillous adenoma with High grade dysplasia